SPIXIANA	48	2	195–213	München, Mai 2026	ISSN 0341-8391

New species of *Pseudogobius* from Qeshm Island, Persian Gulf

(Actinopteri: Teleostei: Gobiidae: Tridentigerinae)

Marcelo Kovačić, Hamid Reza Esmaeili, Golnaz Sayyadzadeh & Vahid Shoaleh

Kovačić, M., Esmaeili, H. R., Sayyadzadeh, G. & Shoaleh, V. 2026. New species of *Pseudogobius* from Qeshm Island, Persian Gulf (Actinopteri: Teleostei: Gobiidae: Tridentigerinae). Spixiana 48 (2): 195–213.

Pseudogobius youtabae sp. nov. is described from Qeshm Island, Persian Gulf. *P. youtabae* sp. nov. is distinguished from congeners by the combination of the following morphological characters: scales in transverse series 7 (non-overlapping vs. 8–12 scales in 6 species); predorsal scales 4–6 (non-overlapping vs. 7–11 in 8 species); operculum with just 2–4 large cycloid scales in 1 or 2 rows (non-overlapping vs. 2–4 rows of more than 4 scales in 14 species); cheek naked (vs. scaly in 2 species); teeth small and similar between rows in both jaws, no sexual dimorphism (non-overlapping vs. 14 species); and coloration pattern (non-overlapping vs. all 15 species). *P. youtabae* sp. nov. differs from the sister species *Pseudogobius minimus* (Hora, 1923) by having scales in transverse series 7; predorsal scale count 4–6; interorbital width 8.4–11.3 % of head length; the first dorsal-fin spine longest in adults, the first spine equal in length to the second spine in juveniles; suborbital sensory papillae row *b* end anteriorly below posterior iris; suborbital sensory papillae row *d* end anteriorly above upper lip near angle of jaws, preorbital rows *jc* and *jd* absent and by coloration details in alive and preserved specimens. The new species has the westernmost distribution of any known *Pseudogobius* species, non-overlapping with other *Pseudogobius* species. *P. youtabae* sp. nov. is also well divergent from the other *Pseudogobius* species by high value (10–23 %) of the K2P genetic distances in the mtDNA COI barcode region being 10 % between *P. youtabae* sp. nov. and *P. minimus*.

Marcelo Kovačić (corresponding author), Natural History Museum Rijeka, Lorenzov prolaz 1, 51000 Rijeka, Croatia; e-mail: marcelo@prirodoslovni.com

Hamid Reza Esmaeili & Vahid Shoaleh, Ichthyology and Molecular Systematics Research Laboratory, Zoology Section, Department of Biology, College of Sciences, Shiraz University, Shiraz, Iran

Golnaz Sayyadzadeh, Department of Biology, Faculty of Sciences, Lorestan University, 6815144316 Khorramabad, Iran

Introduction

The snubnose gobies of the genus *Pseudogobius* Popta, 1922 are small-sized Indo-West Pacific benthic gobies known from estuarine and fresh waters (Larson & Hammer 2021). *Pseudogobius* is a genus in the diverse gobiid subfamily Tridentigerinae (formerly Gobionellinae) according to Larson & Hammer (2021). *Pseudogobius* species are epibenthic on muddy and sandy sediments, seagrass beds, and rocky areas and in mangroves (Larson & Hammer 2021). The genus was recently revised by Larson & Hammer (2021) with description or redescription of all valid species. Among 21 nominal species, they recognized 15 valid species. The distribution of previously described species ranges from eastern Pakistan on the west to the eastern Australia on the east.

Genetic data from both nuclear and mitochondrial markers obtained by Hammer et al. (2021) shed light on inadequacies of the taxonomic framework for the estuarine snubnose gobies of the genus *Pseudogobius*, and the presence of several new taxa in this group in the Indo-West Pacific that were then described by Larson & Hammer (2021). Based on a broad-scale geographic *Pseudogobius* mtDNA comparison between Australian and other areas in the Indo-West Pacific, Hammer et al. (2021) showed significant and major lineage diversity within the morphotypes corresponding to *P. fulvicaudus* Huang, Shao & Chen, 2014 (four lineages from Australia, Malaysia, Singapore and Vietnam) and *P. melanosticta* (Day, 1876) (two lineages, Australia/New Guinea versus Vietnam).

Recently, seven specimens of gobies assigned to the genus *Pseudogobius* were collected from the western part of the Indo-West Pacific in the intertidal coast of the Qeshm Island, Persian Gulf (Fig. 1). Preliminary phylogenetic analyses had revealed that these specimens represent a distinct mtDNA-lineage, which is sister to *P. minimus* (Hora, 1923). The aim of this paper is to describe these specimens as a new cryptic species, *Pseudogobius youtabae* sp. nov., based on their morphological and genetic distinction from other species of the genus *Pseudogobius*.

Materials and methods

Sampling. Specimens were collected from entry of a small estuary with muddy-sandy substrate at Qeshm Island, Persian Gulf (26°41'24.2"N, 55°28'37.9"E), Iran (Fig. 1), using a hand net/scoop net. The fishes were euthanased with an overdose of 1% clove oil solution, photographed and fixed in 10% formaldehyde and later preserved in 70% ethanol. Few specimens were fixed in 96% ethanol and kept at −20°C until DNA extraction.

DNA extraction, PCR and sequencing. For assessing the specific distinctiveness and phylogenetic position of the new species described herein, we sequenced the mitochondrial cytochrome oxidase *c* subunit I (COI) barcode region of three specimens listed in the additional material of the new species (see below). Species identity of these specimens was confirmed by the individual match to the morphological diagnosis. Genomic DNA was extracted from the samples using a SinaPure™ DNA extraction kit (SinaClon Company, Cat. No. EX6011). The mitochondrial COI barcode region was amplified via the polymerase chain reaction (PCR) using the following primers: Partial COI gene sequences were amplified using primer pairs FishF1 (50-TCAACCAACCACAAAGACATTGGCAC-30) and FishR1 (50-TAGACTTCTGGGTGGCCAAAGAATCA-30) (Ward et al. 2005). Amplification was performed on a Bioer XP Thermal Cycler (Bioer Technology Co. Ltd., Hangzhou, China), programmed as following: 94°C for 3 min for initial denaturing, 35 cycles of 94°C for 50 s, 54°C for 45 s, and 72°C for 1 min, followed by 72°C for 5 min as the final extension. Taq DNA Polymerase 2× Master Mix RED (Ampliqon, Cat. No. A180301) was used for PCR reaction. The 25 µl PCR reaction mixes included 12.5 µl of a ready Taq DNA Polymerase 2× Master Mix RED, 0.5 µl of each primer (10 pmol/µl), 5 µl of the target DNA, and 6.5 µl DNase-free distilled water. PCR products were purified using ExoSAP-ITTM and sanger-sequenced by the Niagene Lab. (Tehran, Iran) using Applied BiosystemsTM BigDyeTM Terminator v3.1 Cycle Sequencing Kit on an Applied BiosystemsTM ABI PRISM 3730xl.

Molecular data analysis. Sequence chromatograms were viewed and edited in BioEdit 7.0.4 (Hall 1999). We compiled COI sequence data from 47 representatives of the genus *Pseudogobius* including three sequences of the new species and 44 archived DNA barcode sequences obtained from GenBank and largely derived from the work of Hammer et al. (2021) as given in Table 1. MEGA 6.0 (Tamura et al. 2013) was used to create a DNA sequence alignment by using the Clustal W algorithm. No indications of unexpected stop-codons or nuclear copies of mitochondrial fragments occurred in any sequence. New sequences are deposited in NCBI GenBank (www.ncbi.nlm.nih.gov) with their respective accession numbers (Table 1). The most appropriate sequence evolution model for the given data was determined with a Modeltest (Posada & Crandall 1998) as implemented in jModelTest 2.1.7 (Darriba et al. 2012). To explore species' phylogenetic affinities according to Modeltest, we generated maximum likelihood phylogenetic trees with 10,000 bootstrap replicates using RAxML 7.2.5 software (Stamatakis 2006) under the GTR+I+G model of nucleotide substitution, with fast bootstrap, and also Bayesian phylogenetic analysis (BI) via the Markov Chain Monte Carlo method (MCMC), with 60 000 000 generations under the most generalizing model (GTR+I+G) using MrBayes 3.1.1 (Huelsenbeck & Ronquist 2001). Screening for diagnostic nucleotide substitutions was performed manually from the sequence alignment. Sequence divergence values (Table 2) between species were calculated using the Kimura 2-Parameter (K2P) distance model implemented in MEGA 6.0 (Tamura et al. 2013). As an appropriate outgroup to root the constructed phylogenetic hypothesis, we included the distantly related *Hemigobius hoevenii* (Bleeker, 1851) (accession number: MW498635.1) following Hammer et al. (2021).

Morphology. Measurements were taken with interactively selected points in Olympus cellSens Entry 2.2. software using an Olympus SC180 camera and Olympus U-TV0.5XC-3 camera adapter on an Olympus SZX10 stereomicroscope and with digital calipers. The length of the specimens is presented as standard length (SL) + caudal-fin length. Measurements and counts are selected to be comparable with Larson & Hammer (2021). Morphometric methods, measurements and their definitions follow those of Hubbs & Lagler (1958), as used in

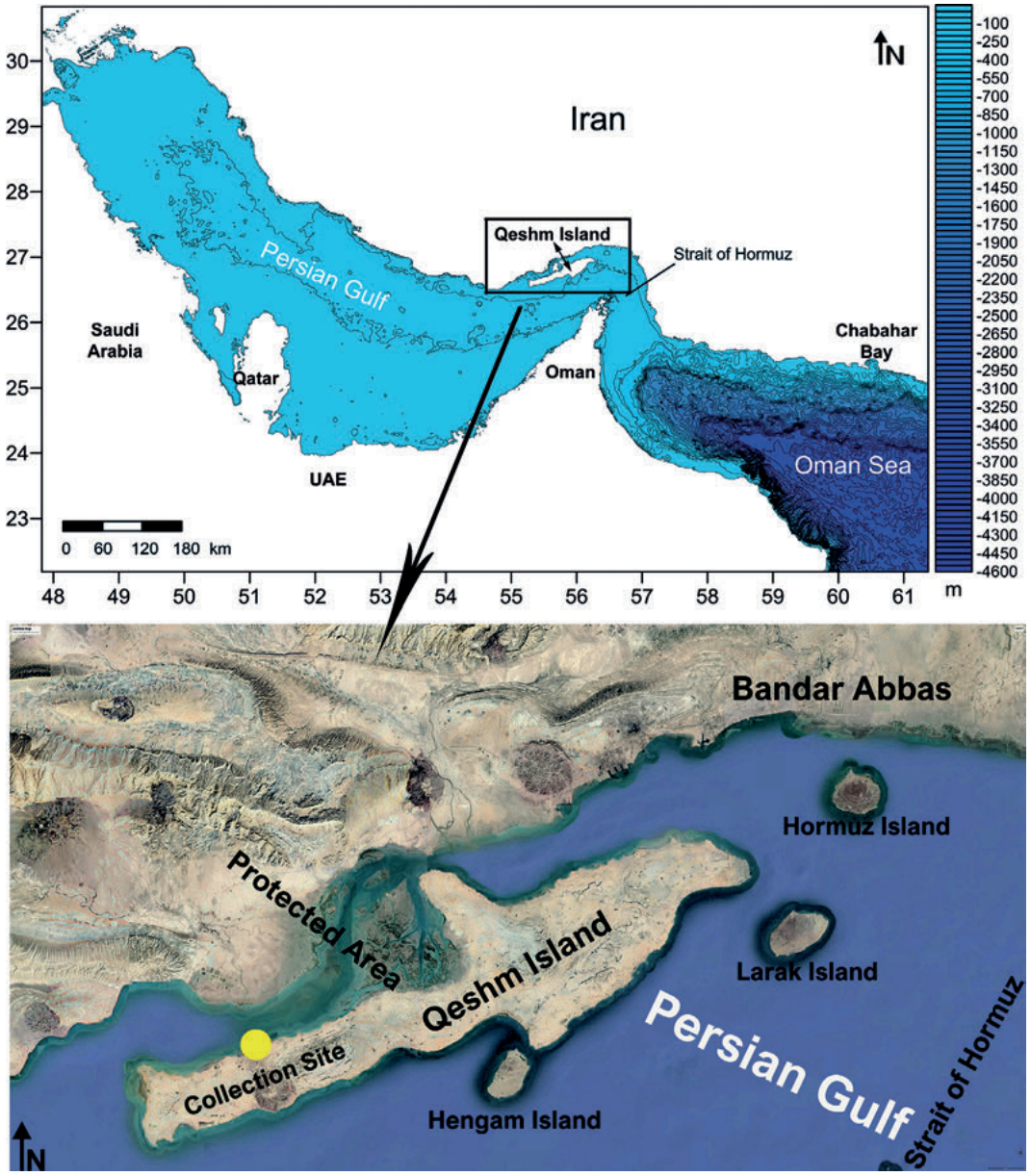

Fig. 1. Type locality of *Pseudogobius youtabae* sp. nov. Iran: Hormuzgan prov., Qeshm Island, Persian Gulf, 26°41'24.2''N, 55°28'37.9''E.

Larson & Hammer (2021). Morphometric data are given as a ratio in the text and as percentages of SL or head length in Table 3. Counts of scales and fins follow Hubbs & Lagler (1958), as used in Larson & Hammer (2021), including transverse scale count and circumpeduncular scale count. Terminology of the cephalic lateral-line system follows Kovačić & Svensen (2024). The material was reversibly stained in a 2 % solution of Cyanine Blue in distilled water (Saruwatari et al. 1997) for the data on squamation, lateral line system and some fin details. Specimens were immersed for 20 seconds in the staining solution. After examination they were returned to original preservative (70 % ethanol) where they reached the original state, i. e. complete loss of any trace of stain-

Table 1. List of DNA sequences taken form GenBank and generated for this study including accession numbers and location.

Species	Accession no.	Locality
P. poicilosoma	KX223937	Malaysia: Pahang, Pekan, South China Sea
P. poicilosoma	MW379463	China: Tokin Gulf, South China Sea
P. poicilosoma	OM311941	India: Kerala
P. poicilosoma	MW379749	China: Tokin Gulf, South China Sea
P. masago	KX223938	Malaysia: Perak, Matang, Malacca Strait
P. masago	KX223939	Malaysia: Pahang, Pekan, South China Sea
P. masago	KX223940	Malaysia: Pahang, Pekan, South China Sea
P. masago	KX223941	Malaysia: Perak, Matang, Malacca Strait
P. masago	MW379733	China: Northern South China Sea, South China Sea
P. fulvicaudus	MW498768	Malaysia: Kedah, Merbok, Semeling Bridge
P. fulvicaudus	MW498769	Malaysia: Kedah, Merbok, Semeling Bridge
P. fulvicaudus	MW498770	Malaysia: Kedah, Merbok, Semeling Bridge
P. olorum	KX223942	Malaysia: Perak, Matang, Malacca Strait
P. olorum	KX223943	Malaysia: Perak, Matang, Malacca Strait
P. olorum	KX223944	Malaysia: Perak, Matang, Malacca Strait
P. olorum	MW498771	Malaysia: Kedah, Merbok, Semeling Bridge
P. olorum	MW498772	Malaysia: Kedah, Merbok, Semeling Bridge
P. olorum	KJ669601	Australia: Finniss River, SA
P. eos	KJ669602	Australia: Georges River, NSW
P. hoesei	MW497079	Australia: Northern Territory, McArthur R.
P. hoesei	MW497081	Papua New Guinea: Pahutuir River
P. hoesei	MW497082	Australia: Northern Territory, Bynoe River
P. hoesei	MW497083	Australia: Queensland, Albert
P. hoesei	MW497085	Papua New Guinea: Port Moresby District
P. hoesei	MW497093	Australia: Queensland, Trunding Creek, Weipa
P. hoesei	MW497094	Australia: Queensland, Trunding Creek, Weipa
P. hoesei	MW497096	Australia: Queensland, Boigu Island, Torres Strait
P. cinctus	MW497084	Australia: Northern Territory, Leaders Creek
P. cinctus	MW497086	Australia: Northern Territory, Blackmore R.
P. cinctus	MW497078	Australia: Northern Territory, Liverpool R.
P. cinctus	MW497092	Australia: Northern Territory, Victoria R.
P. cinctus	MW497101	Australia: Northern Territory, Liverpool R.
P. jeffi	MW497087	Australia: Queensland, Railway drain, Cairns
P. jeffi	MW497088	Australia: Queensland, Bluewater, Cairns
P. jeffi	MW497089	Australia: Queensland, Railway drain, Cairns
P. jeffi	MW497097	Australia: Queensland, Railway drain, Cairns
P. rhizophora	MW497090	Australia: Northern Territory, Middle Beach
P. rhizophora	MW497091	Australia: Northern Territory, Dundee Beach
P. rhizophora	MW497100	Australia: Northern Territory, Maningrida
P. rhizophora	MW497098	Australia: Northern Territory, Maningrida
P. aquilonius	MW497099	Australia: Queensland, Railway drain, Cairns
P. aquilonius	MW497102	Australia: Western Australia, Broome
P. aquilonius	MW497095	Australia: Western Australia, Broome
P. aquilonius	MW497080	Australia: Northern Territory, Vesteys Lake & Creek
P. minimus	OR490927	India
P. minimus	OP034817	Bangladesh
P. youtabae	PX596313	Iran: Hormuzgan prov., Qeshm Island, Persian Gulf
P. youtabae	PX596314	Iran: Hormuzgan prov., Qeshm Island, Persian Gulf
P. youtabae	PX596315	Iran: Hormuzgan prov., Qeshm Island, Persian Gulf

Table 2. Estimates of evolutionary divergence (%) over sequence pairs between species found in the COI barcode region of *Pseudogobius* species studied.

	P. aquilonius	*P. cinctus*	*P. eos*	*P. fulvicaudus*	*P. hoesei*	*P. jeffi*	*P. masago*	*P. melanosticta*	*P. minimus*	*P. olorum*	*P. poicilosoma*	*P. rhizophora*	*P. youtabae*
P. aquilonius													
P. cinctus	13												
P. eos	18	20											
P. fulvicaudus	19	19	22										
P. hoesei	14	12	21	19									
P. jeffi	13	9	19	17	12								
P. masago	20	21	20	20	18	18							
P. melanosticta	20	20	19	21	20	19	19						
P. minimus	20	20	21	22	20	20	13	22					
P. olorum	18	20	14	18	19	17	18	19	21				
P. poicilosoma	21	20	21	21	22	18	21	20	22	19			
P. rhizophora	22	23	18	19	22	20	18	22	21	18	22		
P. youtabae	20	22	23	22	22	20	14	21	10	21	23	22	

Table 3. Morphometric characters (% SL) of *Pseudogobius youtabae* sp. nov. Characters are sorted alphabetically. Morphometric characters with non-overlapping ranges between sexes are marked with * (caudal peduncle depth of the juvenile male slightly overlapping with values of females).

Specimen	PMR VP5875 holotype	PMR VP5876 paratype	PMR VP5877 paratype	PMR VP5878 paratype	PMR VP5879 paratype	ZM-CBSU py001 paratype	ZM-CBSU py002 paratype
Sex	female	female	female	male	male	juvenile female	juvenile male
Standard length	14.9 mm	15.4 mm	14.4 mm	14.0 mm	13.4 mm	11.8 mm	11.7 mm
% of standard length							
Body depth*	16.3 %	15.8 %	15.6 %	17.1 %	17.0 %	15.8 %	16.7 %
Body width*	12.7 %	12.7 %	12.2 %	14.5 %	15.3 %	13.0 %	13.4 %
Caudal fin length	27.2 %	28.9 %	27.9 %	29.0 %	27.0 %	27.2 %	29.5 %
Caudal peduncle depth*	10.8 %	10.2 %	10.4 %	11.1 %	11.4 %	10.9 %	10.8 %
Caudal peduncle length	27.5 %	28.9 %	29.0 %	28.4 %	28.7 %	29.0 %	28.3 %
First dorsal fin depressed	15.6 %	15.3 %	14.8 %	17.7 %	14.5 %	14.7 %	17.0 %
Head length	23.9 %	25.9 %	24.8 %	26.3 %	23.2 %	25.9 %	26.5 %
Pectoral fin length	24.6 %	25.4 %	25.1 %	26.8 %	24.4 %	26.2 %	24.7 %
Pelvic fin length	24.0 %	22.3 %	20.6 %	21.9 %	19.1 %	22.2 %	22.4 %
% of head length							
Eye length	30.3 %	28.3 %	29.1 %	27.5 %	33.2 %	30.4 %	29.0 %
Head depth	63.9 %	62.4 %	62.2 %	63.6 %	68.7 %	64.1 %	58.4 %
Head width	71.4 %	72.2 %	72.3 %	71.4 %	79.7 %	73.9 %	63.2 %
Interorbital width	10.4 %	9.0 %	8.7 %	8.4 %	8.4 %	9.8 %	11.3 %
Snout length	22.4 %	21.1 %	20.7 %	22.4 %	26.5 %	22.5 %	23.2 %
Upper jaw length	33.6 %	31.1 %	27.5 %	26.1 %	28.1 %	24.8 %	29.4 %

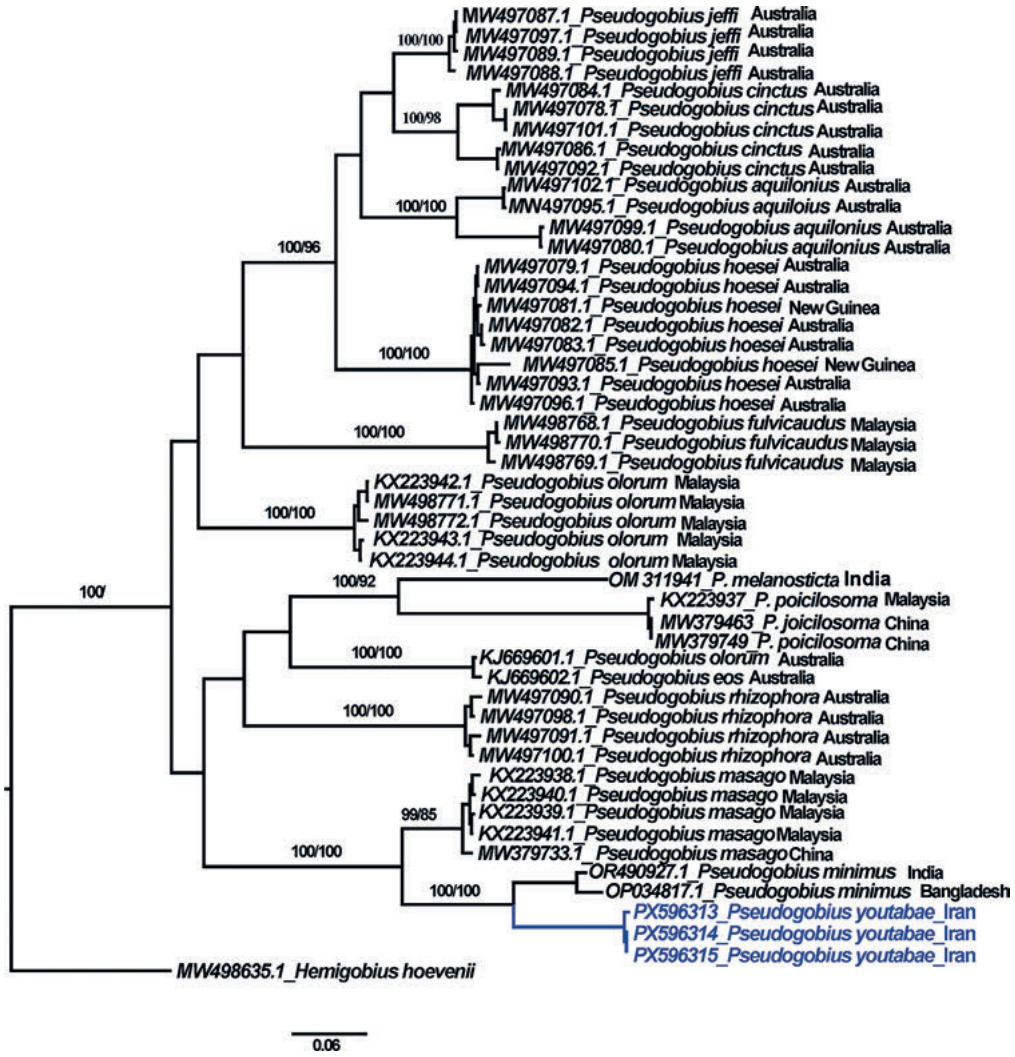

Fig. 2. Maximum Likelihood and Bayesian phylogeny of *Pseudogobius* species reconstructed based on mitochondrial COI gene sequences. The values beside the branches before and after a slash are BI posterior and ML bootstrap probability values, respectively. The ML bootstrap values less than 50 % and posterior probability values less than 95 % are not shown.

ing. The preservative with diluted stain from the specimen was replaced with fresh ethanol 24 hours after staining.

The type material has been deposited at Natural History Museum (PMR), Rijeka, Croatia and the Zoological Museum of Shiraz University, Collection of Biology Department (ZM-CBSU), Shiraz, Iran. No comparative material was studied, considering the well described and illustrated characters in the detailed description of all *Pseudogobius* species that were available in the recent revision of the genus (Larson & Hammer 2021).

Results

Molecular systematics

Both the ML and BI phylogenetic trees were highly similar in their topology, and therefore only the BI tree with posterior probability values complemented by the fast bootstrap values of the Maximum Likelihood RAXML results is presented (Fig. 2). Table 2 contains the average estimates of the evolutionary divergence based on mtDNA COI barcode region among the studied *Pseudogobius* species. The phy-

logenetic tree recovered members of the genus *Pseudogobius* to fall into 11 groups separated by K2P sequence divergence of 9 % (between *P. cinctus* Larson & Hammer, 2021 and *P. jeffi* Larson & Hammer, 2021) to 23 % (between each species of *P. eos* Larson & Hammer, 2021 and *P. poicilosoma*, and *P. youtabae*). Based on the mitochondrial data presented here, *P. youtabae* is sister group to *P. minimus*, and both of them are sister to *P. masago* (Tomiyama, 1936). All six recently described *Pseudogobius* species, i. e. *P. aquilonius* Larson & Hammer, 2021, *P. eos*, *P. hoesei* Larson & Hammer, 2021, *P. cinctus*, *P. jeffi* and *P. rhizophora* Larson & Hammer, 2021, almost match with the results of Hammer et al. (2021). One sequence (KJ669601) identified as *P. olorum* (Sauvage, 1880) is nested in *P. eos*. Hammer et al. (2021) considered *P. olorum* as a complex group forming distinct eastern and western groups, with a relatively narrow contact zone of hybridization.

Generic identification

Complementing the results of molecular phylogenetic analyses, the generic assignment of the new species is also based on morphology. *Pseudogobius youtabae* matches the genus diagnosis in Larson & Hammer (2021), except for the character of predorsal scale count which range should be expanded to "4–11 scales in middorsal row"; the character of sexual dimorphism in dentition which should be excluded from the diagnosis, since in *P. youtabae*, *P. avicennia* (Herre, 1940), *P. masago*, *P. minimus* and *P. rhizophora*, both sexes have similar teeth and no sexual dimorphism was reported (present data, Larson & Hammer 2021); and the character of genital papilla shape which should be excluded from the diagnosis, since papillae of both sexes in *P. youtabae* have unique shapes. The females of the new species had the urogenital papilla rounded, with a longitudinal midventral indentation; the urogenital papilla in males is oval and smooth, with a small opening at the tip, Fig. 3. Based on this, a revised genus diagnosis is provided. The genus *Pseudogobius* differs from other tridentigerines by the following combination of morphological characters (modified from Larson & Hammer 2021): (1) second dorsal fin I,6–9; (2) anal fin I,6–9; (3) second dorsal and anal-fin rays modally equal in number; (4) pectoral-fin rays 14–17; (5) segmented caudal-fin rays 16, often in 9/7 pattern; (6) 24–30 scales in longitudinal series; (7) predorsal scales 4–11, usually with a large scale present close behind eyes (the new species has low predorsal scale count, 4–6); (8) operculum always at least partly scaly (in the new species poorly visible, and scales not visible in the paratype juvenile female ZM-CBSU py001); (9) cheek naked or with 1–3 scales just behind eye; (10) no fine villi on head; (11) posterior portion of oculoscapular canal absent, no preopercular pores; (12) papillae on head in longitudinal pattern, cheek papillae in rows *a*, *c* and *cp* larger and more widely spaced than those in rows *b* and *d*; (13) gill opening restricted to below operculum at most; (14) pectoral girdle smooth or with low flange, without distinct fleshy lobes or flaps; (15) tongue tip blunt to rounded; (16) intestine and stomach coiled in corkscrew manner about each other (the intestine not studied in the new species, since that would destroy the type material morphology); (17) blunt, rounded to inflated snout that may overhang upper lip; (18) lower jaw usually inferior, with jaws usually short with thin to almost absent lips.

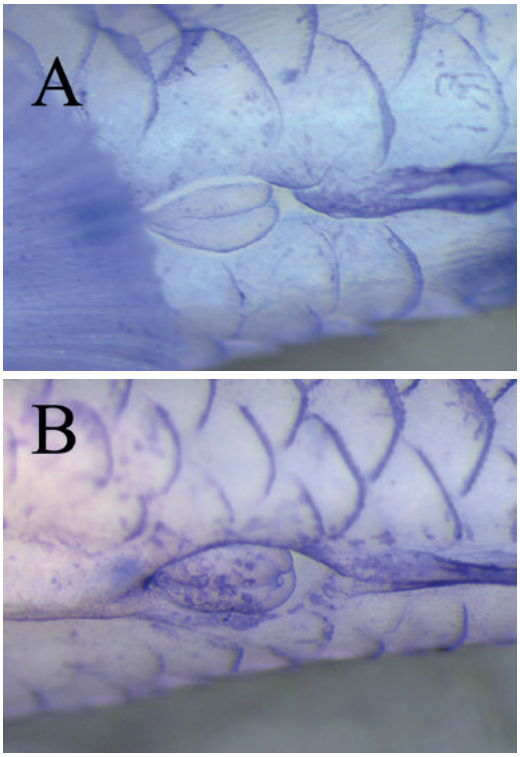

Fig. 3. *Pseudogobius youtabae* sp. nov., urogenital papilla. **A.** female, PMR VP5876, paratype, 15.4 + 4.4 mm; **B.** male, PMR VP5879, paratype, 13.4 + 3.6 mm. Qeshm Island, Persian Gulf. Material reversibly stained, photos by M. Kovačić.

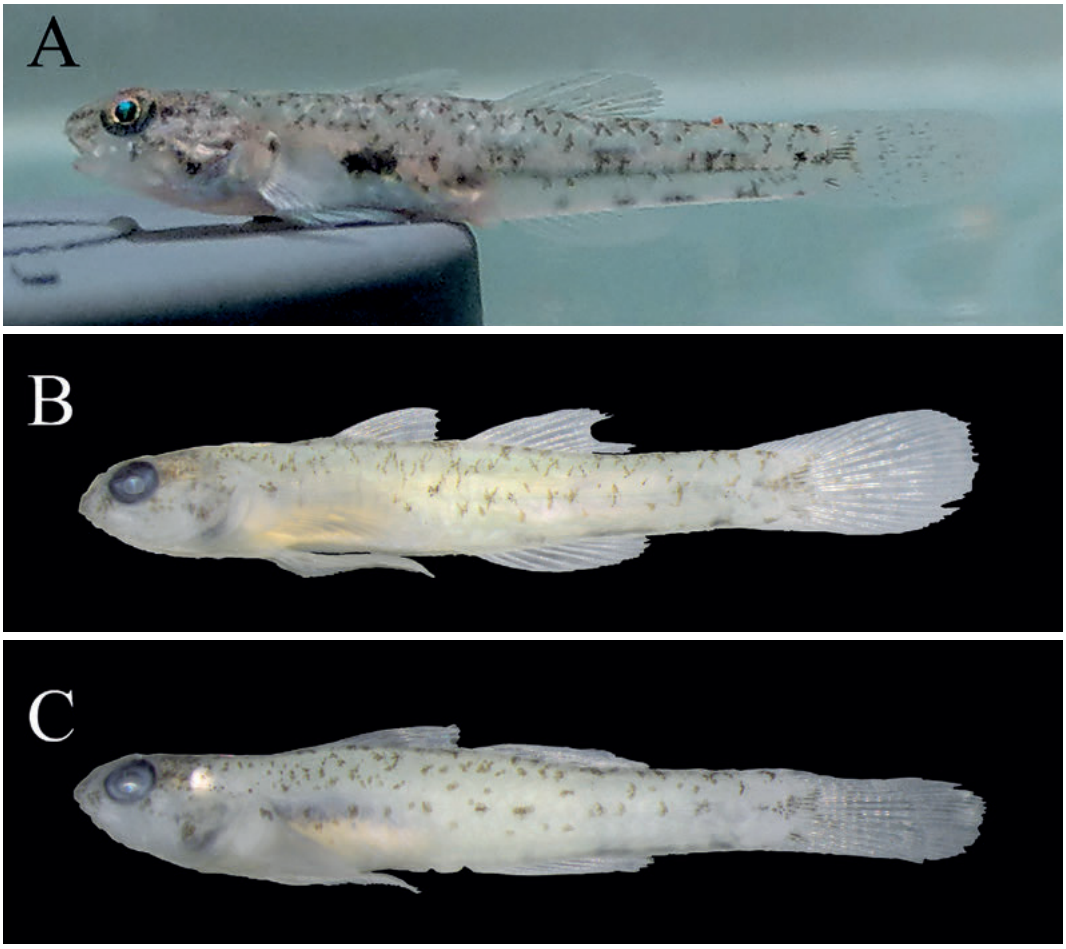

Fig. 4. *Pseudogobius youtabae* sp. nov. **A.** alive specimen from the type material, but individual on the photo not separated and identified among the types, photo by V. Shoaleh; **B.** preserved specimen, PMR VP5875, holotype, female, 14.9 + 4.1 mm; **C.** preserved specimen, PMR VP5879, paratype, male, 14.0 + 4.1 mm. All material from Qeshm Island, Persian Gulf, photos by M. Kovačić.

***Pseudogobius youtabae* sp. nov.**

English name: Youtab Snubnose Goby

Persian name: گوبی درازبینی یوتاب

Fig. 4

Zoobank: http://zoobank.org/urn:lsid:zoobank.org:pub:F01DBC1E-0336-4934-9F09-6C7237828D09

Holotype. PMR VP5875, female, 14.9 + 4.0 mm (Fig. 4B), Persian Gulf, Iran, Hormuzgan prov., Qeshm Island, 26°41'24.2"N, 55°28'37.9"E, collected by Vahid Shoaleh and Yeganeh Sadeghi, 27 Dec. 2022.

Paratypes. PMR VP5876, 15.4 + 4.4 mm; PMR VP5877, female, 14.4 + 4.0 mm; PMR VP5878 male, 14.0 + 4.1 mm (Fig. 4C); PMR VP5879, male, 13.4 + 3.6 mm; ZM-CBSU py001, juvenile female, 11.8 + 3.2 mm; ZM-CBSU py002, juvenile male, 11.7 + 3.5 mm; all data the same as the holotype.

Material for molecular genetic analysis. ZM-CBSU M3654, M3830, M3831; Iran, Hormuzgan prov., Persian Gulf, Qeshm Island, 26°41'24.2"N, 55°28'37.9"E, GenBank accession numbers: PX596313, PX596314, PX596315.

Diagnosis. (1) second dorsal-fin rays I,6–7; (2) anal-fin rays I,6–7; (3) pectoral-fin rays 14–15; (4) segmented caudal-fin rays 15–16, 8–9 upper rays and 7 lower rays; (5) the first dorsal-fin spine longest in adults, the first spine equal in length to the second spine in juveniles; (6) second dorsal-fin and anal-fin

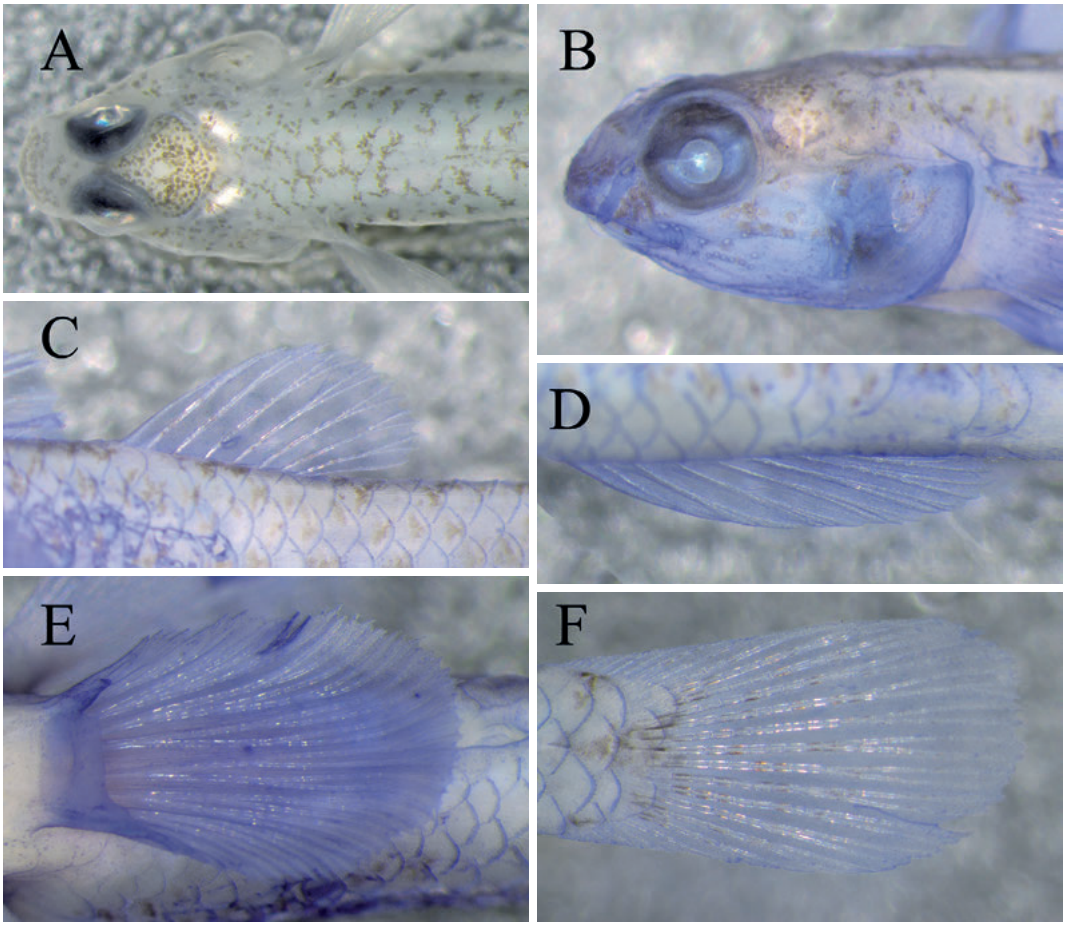

Fig 5. *Pseudogobius youtabae* sp. nov. **A.** predorsal area, PMR VP5877, paratype, female, 14.4 + 4.0 mm; **B.** lateral side of head and pectoral fin base, PMR VP5875, holotype, female, 14.9 + 4.1 mm; **C.** second dorsal fin, PMR VP5876, paratype, female, 15.1 + 4.4 mm; **D.** anal fin, PMR VP5875, holotype, female, 14.9 + 4.1 mm; **E.** pelvic disc and pelvic fin anterior membrane, PMR VP5875, holotype, female, 14.9 + 4.1 mm; **F.** caudal fin, PMR VP5875, holotype, female, 14.9 + 4.1 mm. Qeshm Island, Persian Gulf. Material reversibly stained on photos B-F. Photos by M. Kovačić.

middle rays clearly longer than posteriormost rays (Fig. 5C and D); (7) interorbital width 8.4–11.3 % of SL; (8) longitudinal scale series 26–30; (9) transverse scales 7; (10) predorsal scales 4–6; (11) opercle with 2–4 cycloid scales, cheek naked; (12) shoulder girdle smooth; (13) tongue short with blunt tip; (14) teeth small and similar between rows in each jaw, no sexual dimorphism; (15) suborbital sensory papillae row *b* ending anteriorly below posterior iris; (16) suborbital sensory papillae row *d* anteriorly ending above upper lip near angle of jaws, preorbital rows *jc* and *jd* absent; (17) in fresh individuals head and body translucent whitish to pale whitish grey, with visible vertebrae, dark abdominal pigmentation and silvery peritoneum; (18) preserved and alive specimens without pigmentation below midlateral spots, except for a row of three to four grey internal dashes above the anal fin and on the caudal peduncle; (19) in preserved and alive specimens of both sexes, the midlateral brown marks are just slightly more obvious than the upper body scale margin outlines, except for the posteriormost spot at the center of caudal-fin base; (20) in preserved and alive specimens of both sexes, body with the scale margins above lateral midline partially outlined with brown pigmentation (Fig. 4); (21) in preserved and alive specimens of both sexes, lower half of head whitish with no pigmentation (Figs 4 and 8D);

(22) in preserved and alive specimens of both sexes, first and second dorsal fin with a few brown dashes along rays present or absent, the rest of fins transparent (Figs 4 and 8E); (23) in preserved specimens and alive specimens of both sexes, the mark on the base of lowermost caudal-fin rays poorly visible (Figs 4 and 8B); (24) preserved and alive specimens of both sexes with a small brown mark at upper pectoral-fin base.

Description

(all morphometrics and meristics in the text are presented for the holotype first and paratypes in parentheses)

General morphology. (Fig. 4) Body proportions are given in Table 3. Body slender, its depth at anal-fin origin 6.1 (5.9–6.0 in male paratypes, 6.3–6.4 female paratypes) in SL, body width 7.9 (6.5–7.4 in male paratypes, 7.7–8.2 in female paratypes) in SL, posteriorly progressively laterally compressed, with caudal peduncle elongate, slender and laterally compressed, caudal peduncle length in SL 3.6 (3.4–3.7), caudal peduncle depth in SL 9.3 (8.8–9.3 in male paratypes, 9.2–9.8 in female paratypes), depth in caudal peduncle length 2.6 (2.5–2.8) (Fig. 4). Head moderately small, wide, the length 4.2 (3.8–4.3) in SL, width 1.4 (1.3–1.6) in head length, depth 1.6 (1.5–1.7) in head length, and slightly depressed, its depth at posterior preopercular margin in width at posterior preopercular margin 1.1 (1.1–1.2). Postorbital profile nearly horizontal. Cranial roof covered partially by dorsal axial musculature, behind eyes large diamond shaped surface without dorsal axial musculature, covering entire distance between eye and posterior edge of preopercle (Fig. 5A). Snout blunt and rounded, well overhanging upper lip, shorter than eye diameter, its length 1.4 (1.2–1.3 in male paratypes, 1.4 in female paratypes) in eye diameter, 4.5 (3.8–4.8) in head length (Fig. 5B). Anterior nostril a very short tube, directed downwards over upper lip. Posterior nostril a rounded opening, with very low rim, placed near eye at mid-level of eye (Fig. 5B). Eyes dorsolateral, upper edge of eye forming part of dorsal profile and not extending above it, eye diameter 3.3 (3.0–3.6) in head length. Interorbital area narrow (Fig. 5A), 2.9 (2.6–4.0) in eye diameter, 9.7 (8.9–11.9) in head length. Mouth small, subterminal, slightly oblique, upper jaw slightly overhanging lower jaw (Fig. 5B); jaws posteriorly reaching to vertical through anterior edge of pupil; upper jaw 3.0 (3.2–4.0) in head length; lips relatively thin, lower lip fleshier than upper and fused to chin anteriorly (Fig. 5B). Cheek moderately deep. Chin without mental fold. Teeth hard to see, hidden by flesh except for the tips. No sexually dimorphic dentition. Upper-jaw teeth in 2–3 rows, very small; teeth in outer row slightly larger. Lower-jaw teeth in 2–3 rows, very small. Tongue short, with blunt and truncate tip. Branchiostegal membrane attached along lateral margin of isthmus to below half of operculum. No spines on preopercle. Pectoral girdle smooth. Urogenital papilla in females rounded, with bifurcated posterior edge, longitudinal midventral indent and opening hidden in indent close to the tip (Fig. 3A), in paratype juvenile female ZM-CBSU py001 the indent is less prominent. Urogenital papilla in males oval and smooth, with small opening visible at the tip (Fig. 3B).

Fins. First dorsal fin VI (VI), second dorsal fin I,7 (I,6: 1, I,7: 5); anal fin I,7 (I,6: 1, I,7: 5); caudal-fin rays (as upper + lower): segmented caudal-fin rays 9 + 7 (8 + 7: 4, 9 + 7: 2), branched caudal-fin rays 7 + 6 (6 + 6: 1, 7 + 6: 5), procurrent caudal-fin rays 8 + 6 (7 + 7: 2, 8 + 7: 3, paratype juvenile female ZM-CBSU py001 not clear for count); pectoral-fin rays, left and right: 15 and 15 (14 and 14: 3, 15 and 14: 2, 15 and 15: 1), pelvic fins I,5 (I,5). Fin morphometrics in proportion to standard body length given in Table 1. Spines of first dorsal fin not elongate or filamentous, the first to third spine subequal in length, first spine longest, 13.4 % (11.8–16.7 %) of SL, except in paratypes female PMR VP5876 and juvenile male ZM-CBSU py002, where first spine equal in length to the second spine, second spine 12.3 % (11.5–16.0 %) of SL, third spine 11.8 % (10.8–14.7 %) of SL, remaining spines progressively decreasing in length. Spines of first dorsal fin not reach the origin of second dorsal fin when folded down. Origin of first dorsal fin behind vertical at pectoral-fin base. Interdorsal space relatively broad, membranous connection between dorsal fins absent, with membrane of the first dorsal fin covering about half of distance between sixth spine of the first dorsal fin and the first spine of the second dorsal fin (Fig. 5C). Second dorsal and anal fin moderate in height, both fins rounded posteriorly (Fig. 5C and D). Second dorsal-fin middle rays clearly longer than posteriormost rays, rays 2 and 3 the longest, 15.1 % (12.5–14.4 %) of SL, (Fig. 5C). Second dorsal-fin anterior origin behind vertical of anus, with the posterior rays when folded down end distant from the base of uppermost caudal-fin rays, covering about $^2/_5$ of distance between last anal-fin ray and the first procurrent caudal-fin ray, about $^1/_3$ in juveniles. Anterior origin of anal fin below the base of the second dorsal-fin spine or the first dorsal-fin ray. Anal-fin middle rays clearly longer than posteriormost rays, second to fourth rays longest, 12.6 % (10.7–13.5 %) of SL (Fig. 5D). Base of last anal-fin ray below the base of the last dorsal-fin ray. Anal-fin posterior rays, when appressed, end distant from the base of lowermost caudal-fin rays,

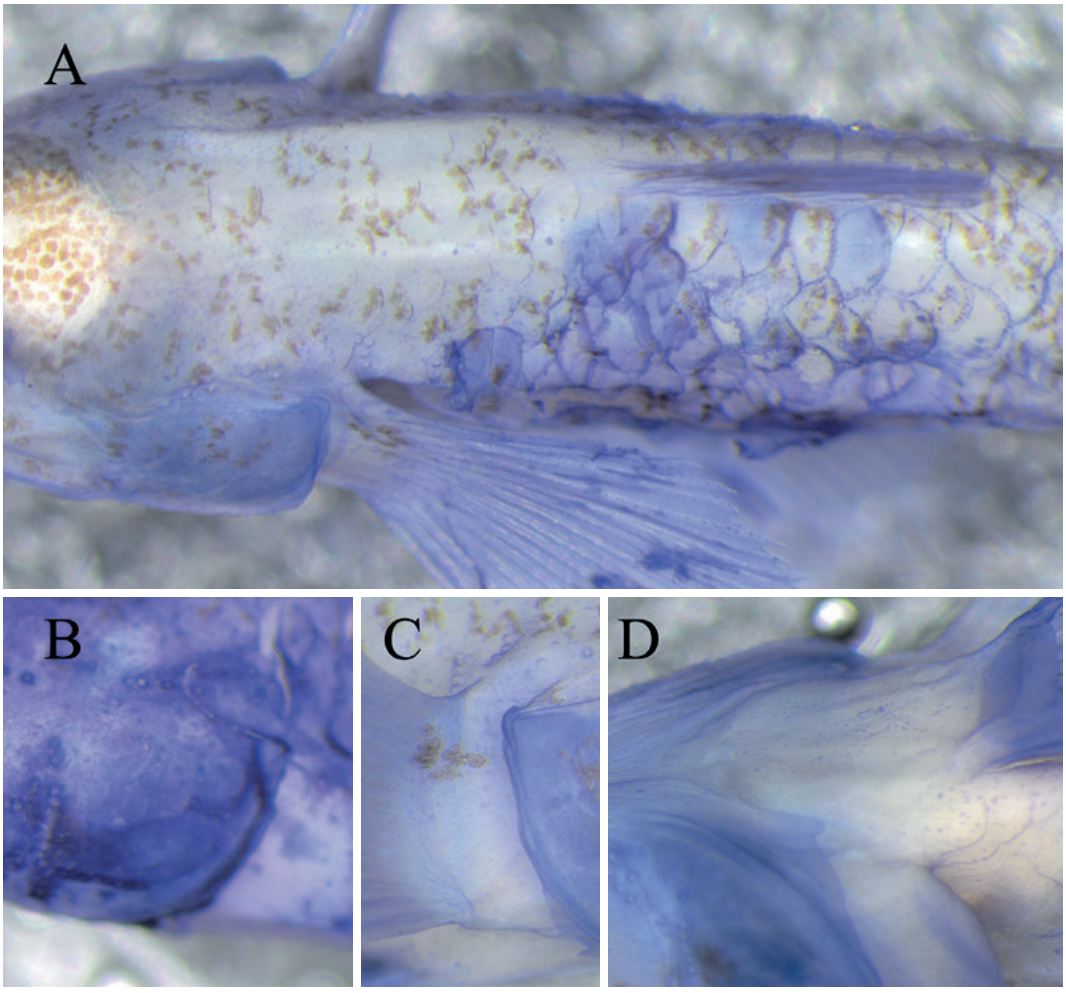

Fig 6. *Pseudogobius youtabae* sp. nov. **A.** predorsal area and the first dorsal-fin fin base, PMR VP5875, holotype, female, 14.9+4.1 mm; **B.** operculum, ZM-CBSU py001, paratype, juvenile male, 11.7+3.5 mm; **C.** prepectoral, PMR VP5875, holotype, female, 14.9+4.01 mm; **D.** prepelvic area, PMR VP5875, holotype, female, 14.9+4.1 mm. Qeshm Island, Persian Gulf. All material reversibly stained. Photos by M. Kovačić.

$^{2}/_{5}$ of distance between last anal-fin ray and the first procurrent caudal-fin ray, about $^{1}/_{3}$ in juveniles. Pectoral-fin all branched or only uppermost and lowermost rays not branched, upper rays not free at tips. Pectoral fins large, rhomboid, central rays longest, extending to vertical above anus, 4.07 (3.73–4.10) in SL. Pelvic disc complete, oval, with rounded posterior margin, all rays branched, fifth ray longer than fourth ray; pelvic frenum well-developed, in midline width about $^{2}/_{3}$ of spinous ray, with smooth edge (Fig. 5E). Pelvic fins 4.17 (3.73–4.10) in SL, nearly reaching to anus in males, in adult females reaching anus, but not reaching urogenital papilla, reaching urogenital papilla only in paratype juvenile female ZM-CBSU py001. Caudal fin broad, rounded posteriorly (Fig. 5F); caudal fin longer than head, 0.88 (0.86–0.95) in head length.

Scales. Body covered with ctenoid scales on flanks and along bases of unpaired fins. Scales in longitudinal series: right side 26, left damaged for count (both sides 27:1, 28:5, 29:1, 30:2, not counted left side in paratype male PMR VP5879 and both sides in paratype juvenile female ZM-CBSU py001 due to surface damage, ZM-CBSU py001 with too damaged scales and scale pouches on caudal peduncle for count, even after staining), with one or two more rows of scales extending past base of the caudal-fin rays not counted (Fig. 5F). Scales counted longitudi-

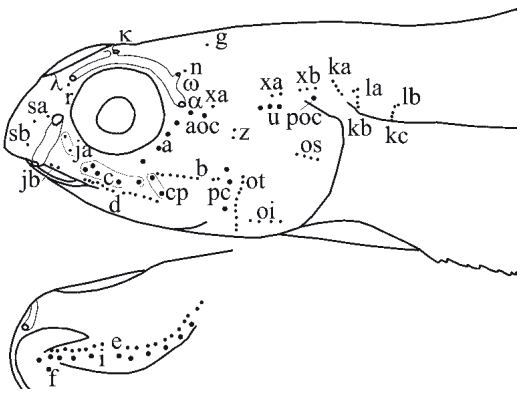

Fig. 7. *Pseudogobius youtabae* sp. nov. Head lateral line sensory papillae and canal pores: PMR VP5875, holotype, female, 14.9 + 4.1 mm, Qeshm Island, Persian Gulf. Terminology in text. Drawing by M. Kovačić.

nally from behind pectoral axilla: right side 24, left damaged for count (both sides 25: 2, 26: 4, 27: 3, not counted on left side in paratype male PMR VP5879 and both sides in paratype juvenile female ZM-CBSU py001 due to the surface damage) with one or two more row of scales extending past base of the caudal-fin rays not counted. Scales in transverse series right side 7, left damaged for count (7: 11, left side in paratype male PMR VP5879 not counted due to the surface damage). Scales in circumpeduncular series 10 (both sides 11: 5, not counted in paratype juvenile female ZM-CBSU py001 due to the surface damage on caudal peduncle). Uppermost and lowermost scales at caudal-fin base not elongate, all caudal-fin scales with very short ctenii, almost cycloid (Fig. 5F). Head with cheek naked and operculum with just two to four poorly visible large cycloid scales in 1 or 2 vertical rows (Fig. 6B), not visible in juvenile female ZM-CBSU py001. Predorsal area at middorsal scaled to above pectoral-fin base or slightly forward, except for holotype female PMR VP5875 where scales extend above vertical to operculum (predorsal scales poorly visible even with the stain but the posterior edges of two anterior middorsal scales above operculum poorly visible on Fig. 6A), laterally predorsal scaled to above pectoral-fin base, the area between the origin of the first dorsal fin and vertical of pectoral-fin base more or less scaled, predorsal scale count 6 (4: 3, 5: 3) (predorsal scales poorly impregnated with the stain but the posterior scale edges visible on Fig. 6A). The entire first and second dorsal-fin base scaled (Fig. 6A). Prepectoral area naked (Fig. 6C). Pectoral axilla naked. Breast naked (Fig. 6D). Belly covered entire with cycloid scales, except the anterior area just behind pelvic axilla that is naked.

Cephalic lateral-line system (Fig. 7)**.** The rows of head sensory papillae were counted on the left side of all type specimens. Head lateral-line system with anterior oculoscapular canal without posterior part, with interorbital pores λ and κ, and pores ω and α behind eye. The pores λ paired, the pore κ median, single. Posterior oculoscapular and preopercular canals absent. Holotype female PMR VP5875 and paratype male PMR VP5879 with aberration of doubled pores ω on the left side. The paratype juvenile female ZM-CBSU py001 with not completely formed canal, anteriormost and posteriormost pores λ and α well defined, but the central part of the canal still open as furrow. Head rows of sensory papillae with low papillae counts in rows, some rows with just one or two papillae or absent. *Preorbital* rows with three median rows reduced to one or two papillae. Longitudinal row *r* a single papilla located anteriorly below pore λ; transverse row *sa* (1–2) medially to posterior nostril, row *sb* (1–2) medially to interspace between anterior and posterior nostrils; row *sc* as the anteriormost *preorbital* row above upper lip not visible. Two lateral *preorbital* rows. Row *ja* (2–3) as distantly scattered papillae laterally to between anterior and posterior nostrils; transverse row *jb* (1-2) laterally close to anterior nostril; two lowermost rows, superior row *jc* and inferior row *jd*, absent. *Suborbital* rows without transverse proliferation, cheek papillae in rows *a*, *c* and *cp* larger and more widely spaced than those in rows *b* and *d*. Row *a* restricted at ventroposterior part of eye (3–4); row *b* (9–10) extending from below posterior margin of eye to near preopercular edge, ending between *pc* papillae, in holotype female PMR VP5875 and paratype juvenile male ZM-CBSU py002 divided in two parts; row *c* (5) below anterior eye and mideye, anteriorly starting with three papillae in triangular shape, one above and two below; row *cp* oblique, below row *b* as two papillae one above other; row *d* (9–15) extending from above upper lip near angle of jaws, posteriorly to vertical of posterior margin of eye or near it, in holotype female PMR VP5875 and paratypes female PMR VP5877 and in juvenile male ZM-CBSU py002 divided below mideye. *Preoperculo-mandibular* rows with external row *e* (8 + 8 to 7 + 13) and internal row *i* (5 + 5 to 6 + 8) divided, row *i* parallel to row *e*, both ending anteriorly at chin behind front of jaw, row *i* more anteriorly, both ending posteriorly at preopercular ventral margin, row *e* more posteriorly. Mental row *f* as single papilla near chin tip behind anterior end of row *i*. *Opercular* rows with two or three larger papillae *pc* on the place of the missing preopercular canal; transverse row *ot* positioned anteriorly on operculum (9–14); superior longitudinal row *os* in upper posterior part of operculum (3–5); inferior longitudinal row *oi* on lower part of operculum

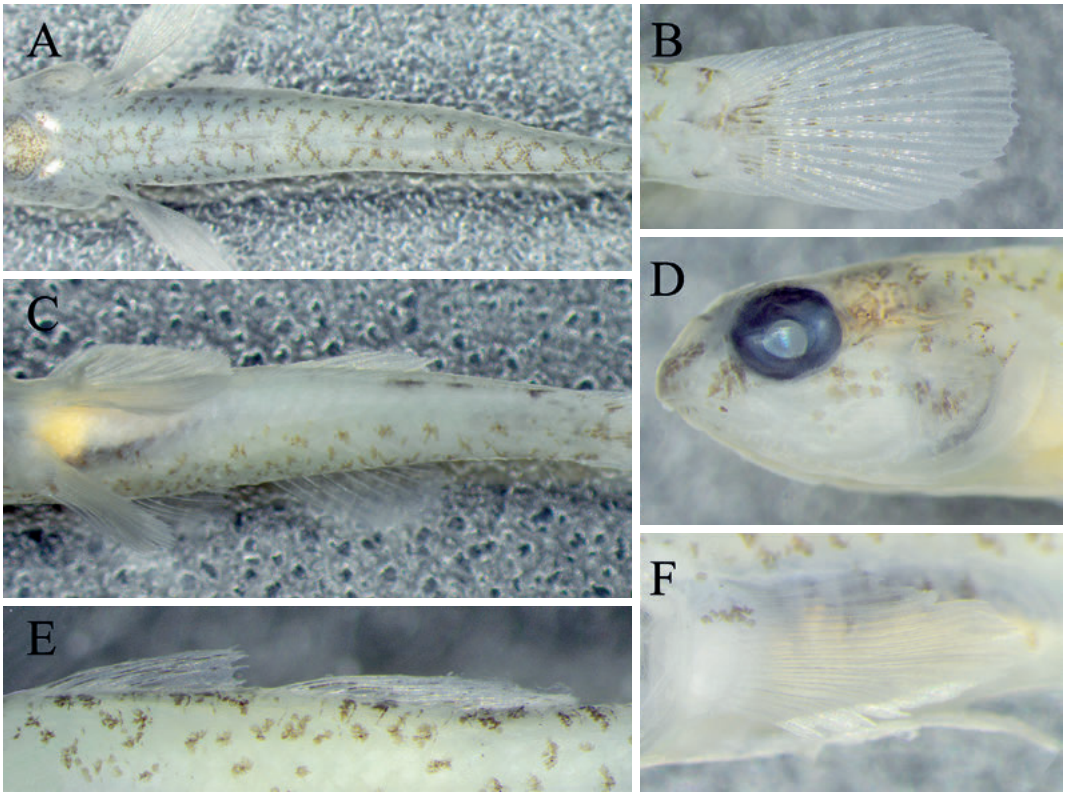

Fig. 8. *Pseudogobius youtabae* sp. nov. **A.** dorsal side, PMR VP5877, paratype, female, 14.4 + 4.0 mm; **B.** caudal fin, PMR VP5875, holotype, female, 14.9 + 4.1 mm; **C.** ventral side, PMR VP5876, paratype, female, 15.4 + 4.4 mm; **D.** head, PMR VP5875, holotype, female, 14.9 + 4.1 mm; **E.** dorsal fins, PMR VP5878, paratype, male, 14.0 + 4.1 mm; **F.** pectoral fin, PMR VP58773, paratype, female, 14.4 + 4.0 mm. Qeshm Island, Persian Gulf. Photos by M. Kovačić.

(3–8). *Oculoscapular* rows with larger *aoc2* papillae (2–3) behind pore α on the place of the missing posterior part of anterior oculoscapular canal. Anterior longitudinal row *xa* (1 + 2 to 5 + 4) divided into anterior part above preopercule and posterior part above anterior operculum; posterior longitudinal row *xb* (2–4) above posterior edge of operculum, not visible in paratype female PMR VP5876. Row *z* (2–3) present in the area of upper preopercular edge, not visible in about half of specimens. Row *q* absent. Row *u* as three papillae above anterior operculum and below posterior part of row *xa*, only two visible in paratype male PMR VP5879. Row *y* absent. Single larger *poc* papilla above posterior edge of operculum and below row *xb* on the place of the missing posterior oculoscapular canal, not visible in paratypes female PMR VP5877 and male PMR VP5878. Transverse axillary rows *ka* (3–4), *kb* (3–4) and *kc* (3–7) radiating from upper pectoral-fin base; axillary rows *la* (1–3) and *lb* (2–3) oblique, just above rows *kb* and *kc*, respectively, row *lb* not visible in paratypes female PMR VP5877 and juvenile female ZM-CBSU py001. *Anterior dorsal* rows with row *n* on anterior nape behind eye and just behind lower pore ω as a single papilla. On the place of papillae *o*, *g* and *m* only one papilla visible, not visible in paratype female PMR BP5877, and as two papillae in paratypes male PMR VP5879 and juvenile female ZM-CBSU py001. Longitudinal row *h* near dorsal midline in front of first dorsal fin origin as single papilla, not visible in about half of the individuals, including holotype. *Interorbital* rows absent.

Coloration. Colour of alive specimens (from the photos of alive individuals, Fig. 4A). Head and body translucent whitish to pale whitish grey, with visible vertebrae, silvery peritoneum and dark abdominal pigmentation between vertebrae and silvery peritoneum. Vertebrae with dark thin outline, more consistent ventrally than dorsally. The scale margins above lateral midline at least partially outlined with greyish brown. Midlateral spots recognizable just as slightly more intensive greyish brown marks

than other scale margin outlines. Posteriormost spot at middle of caudal-fin base greyish brown, horizontally elongate, extending backward onto caudal fin, larger than other midlateral spots, this spot preceded by a small black spot as large as half pupil diameter. Ventral side of body whitish with no pigmentation, except for the longitudinal row of three to four grey internal dashes above anal fin and on caudal peduncle. Upper half of head from snout to operculum pigmented. Cheek with a greyish brown band from eye to upper lip. Brown mark below posterior eye present in some individuals. Lower half of head, breast and belly whitish without pigmentation. First and second dorsal fin with a few brown dashes along rays, the rest of fins transparent. Anal fin translucent. Pectoral fin with small brown mark at base of upper fin rays and white pigments along lower fin rays. Pelvic fins translucent. Caudal fin transparent with few melanophores along rays and the extension of caudal-fin base spot onto the origin of middle rays.

Colour of preserved specimens (Fig. 4B and C). No visible sexual dichromatism, females and male with head and body whitish to yellowish. Scale margins above lateral midline partially outlined with brown pigmentation, only a few brown spots scattered below lateral midline. In smaller specimens scale margin pattern reduced to individual brown dots, losing reticulate pattern. From top view five pale saddles with almost no melanophores recognizable on dorsal side, four at start and end of each dorsal fin base and a fifth, less recognizable, on caudal peduncle (Fig. 8A). Midlateral spots recognizable just as slightly more prominent brown marks than other scale margin outlines (Figs 4 and 8C). Posteriormost spot at middle of caudal-fin base as a brown blotch, larger than other midlateral spots, roughly triangular or just irregularly elongate, pointed anteriorly and extending backward and up onto base of three to five caudal-fin rays just above midline (Fig. 8B). Ventral side of body whitish with no pigmentation, except for two or three dark dashes along midventral area, less visible in juveniles on caudal peduncle and dark dash or brown mark at middle of anal fin base, the last visible in holotype female PMR VP5875 and paratype female PMR VP5877 (Fig. 8C). Top of head behind eye dusky brownish with densely scattered melanophores, brains visible below as yellow mass and in smaller specimens also otoliths as two comparatively bright oval areas posterolaterally of brain (Fig. 5A). The predorsal behind just with a few scattered melanophores like on other parts of the body (Fig. 5A). Snout with two transverse diffuse brown stripes, at frontal edge of eyes and above upper lip in larger individuals, only as scattered melanophores in smaller specimens. Cheek with brown band from eye to upper lip (Fig. 8D). Brown mark below posterior eye present in preserved individuals only in paratype female PMR VP5876. Upper part of cheek behind eye and operculum with a faint brown stripe, reduced to a few scattered melanophores in smaller specimens (Fig. 8D). Lower half of head whitish with no pigmentation. Underside of head, breast and belly whitish. First and second dorsal fin with a few brown dashes along rays present or absent, the rest of fins transparent (Fig. 8E). Anal fin translucent (Fig. 8C). Pectoral fin transparent with small brown mark at pectoral base of upper rays 2 or 3 to rays 5 or 6, narrower in juveniles (Fig. 8F). Pelvic fins translucent. Caudal fin transparent with the extension of the caudal fin base spot onto the origin of middle rays and a poorly visible mark below it on the base of lower cauda-fin rays (Fig. 8B). The rest of the fin with a few melanophores along rays (Fig. 8B).

Etymology. The species is named after Youtab, meaning "unique" in Old Persian (4th century BC–330 BC). Youtab was an ancient Persian noblewoman. She was the sister of Ariobarzanes, Satrap of Persis. She is known for fighting alongside her brother against the Macedonian King Alexander the Great at the Battle of the Persian Gate in the winter of 330 BC.

Distribution and ecology. *Pseudogobius youtabae* is presently only known from the intertidal zone at the coast of Qeshm Island, Persian Gulf (Figs 1 and 9). The species was found during low-tide at early hours of the day when the temperature of the water was cooler than later in the daytime, at a depth of 0–0.5 meters on a sandy-muddy substrate, with the grey colour it could camouflage greatly because of the grey background colour. Day's goby *Acentrogobius dayi* Koumans, 1941 was one of the main sympatric fish species and the juvenile of this species can be confused with *Pseudogobius* specimens in the field.

Remarks. Among 15 valid species of *Pseudogobius*, the counts of the new species overlap with all of them for the fin meristics and in count of scales in longitudinal series, i.e. with regard to five of the characters that were used in the diagnoses of *Pseudogobius* species (Larson & Hammer 2021). The overlap is common in the genus and these characters are of no use in almost any compared pair among *Pseudogobius* species. Two other characters derived from Larson & Hammer (2021), i.e. the shoulder girdle and the tongue size and shape, had the same lack of difference among *Pseudogobius* spp. The shoulder girdle is smooth in all or at least in some specimens of all *Pseudogobius* species, including the presently described species, except *P. jeffi* (Larson & Hammer 2021). The tongue was described "short" or "short to greatly reduced" or "reduced", in all

Fig. 9. Natural habitat (type locality) of *Pseudogobius youtabae* sp. nov., Hormuzgan prov., Qeshm Island, Persian Gulf. Photo by V. Shoaleh.

Pseudogobius species, with a blunt tip in all or in at least some specimens of all species, including the presently described species (Larson & Hammer 2021). Nevertheless, all original 13 characters of species diagnoses used in the genus revision by Larson & Hammer (2021) were kept in the present diagnosis to keep it comparable with past and future *Pseudogobius* species descriptions or redescriptions. The remaining six diagnostic characters of squamation, dentition and coloration from Larson & Hammer (2021) well differentiate many *Pseudogobius* species pairs. Character states of those six characters in the diagnosis of *P. youtabae* distinguish the new species from all congeners by three (6 species), four (4 species) or five characters (5 species) to each compared species: i. e. the low count of scales in transverse series 7 (non-overlapping vs. 8–12 scales in 6 species); the low longitudinal median count of predorsal scales 4–6 (non-overlapping vs. 7–11 scales in 8 species); operculum with just 2–4 scales in 1 or 2 rows (non-overlapping vs. more than 4 scales in 2–4 rows in 14 species); cheek naked (non-overlapping vs. 2 species); teeth small and similar between rows in both jaws, no sexual dimorphism (non-overlapping vs. 14 species); coloration pattern was non-overlapping vs. all 15 species (Table 4). Other *Pseudogobius* species have brown skin pigmentation present below lateral midline. Most of them have more intense brown pigmentation in general, compared to *P. youtabae* and also many of them have individual coloration marks on body that are species specific, each of them lacking in *P. youtabae*. The exception is closely related *P. minimus*, which is distinguished from the new species by having an even less pigmented body than *P. youtabae*, i. e. missing several marks present on the new species: *Pseudogobius youtabae* differs in coloration of preserved specimens and alive specimens of both sexes from *P. minimus* by melanophores connected to form midlateral brown marks in alive and preserved individuals vs. melanophores at midlateral at best grouped as individual, distinct and separate dots in *P. minimus*; by a small brown mark at the upper pectoral-fin base vs. melanophores at upper pectoral-fin base grouped as individual distinct dots in *P. minimus*. In addition to coloration, *P. youtabae* is distinguished from its phylogenetically sister species *P. minimus* (Fig. 2) by the following morphological characters (present

Table 4. The six scales, teeth and coloration characters that are differential with regard to pairwise *Pseudogobius* species comparisons (the data on the new species from present research, others from Larson & Hammer 2021).

Species	Transverse scale count	Predorsal scale count	Operculum scales	Cheek scales
Pseudogobius youtabae sp. nov.	7	4 to 6	2–4 large cycloid scales in 1-2 rows	Cheek naked
Pseudogobius aquilonius Larson & Hammer, 2021	7 to 9	6 to 8	2 or more rows of cycloid scales	Cheek usually naked
Pseudogobius avicennia (Herre, 1940)	6 to 8 1/2	8 to 10	2–4 rows of cycloid scales	Cheek naked
Pseudogobius cinctus Larson & Hammer, 2021	7 to 8 1/2	7 to 8	3 rows of cycloid scales	1–2 cycloid scales
Pseudogobius eos Larson & Hammer, 2021	8	7 to 10	Several rows of small cycloid scales	Cheek usually naked
Pseudogobius fulvicaudus Huang, Shao & Chen, 2014	7 to 8	6 to 7	2–4 rows of cycloid scales	Cheek naked
Pseudogobius hoesei Larson & Hammer, 2021	7 to 8	6 to 7	Several rows of cycloid scales	Cheek naked
Pseudogobius jeffi Larson & Hammer, 2021	7 to 9	6 to 7	3 rows of large cycloid scales	Single cycloid scale
Pseudogobius masago (Tomiyama, 1923)	7 to 8	7 to 10	2 or more rows of cycloid scales	Cheek naked
Pseudogobius melanosticta (Day, 1876)	8 to 10	6 to 8	2–4 rows of ctenoid scales	Cheek naked
Pseudogobius minimus (Hora, 1923)	8	8 to 10	1 to 2 rows of cycloid scales	Cheek naked
Pseudogobius olorum (Sauvage, 1880)	8 to 12	8 to 11	Several rows of small cycloid scales	Cheek naked
Pseudogobius poicilosoma (Bleeker, 1849)	7 to 10	6 to 8	2 or more rows of cycloid scales	Cheek usually naked
Pseudogobius rhizophora Larson & Hammer, 2021	8 to 9	6 to 8	3 rows of cycloid scales	Cheek naked
Pseudogobius taijiangensis Chen, Huang & Huang, 2014	8 1/2 to 9	8 to 9	3–4 rows of cycloid scales	Cheek naked
Pseudogobius verticalis Larson & Hammer, 2021	7 to 9	6 to 7	3–4 rows of cycloid scales	Cheek naked

Upper jaw teeth	Body coloration in alive and preserved individuals
Upper jaw teeth in 2–3 rows, similar between rows and very small in both sexes.	No pigmentation below midlateral spots, except for row of three to four grey internal dashes above anal fin and on caudal peduncle. Melanophores connected into midlateral brown marks.
Upper jaw teeth in 3–4 rows. In males teeth in outer row slightly flattened, blunt-tipped or pointed; in females, outer row teeth small, compressed and blunt-tipped; teeth in inner rows always very small, close-set and sharp.	Skin pigmentation below midlateral spots present.
In both sexes upper jaw teeth in 2 rows, teeth in outer row pointed, bluntly rounded to flattened, small, closely spaced, evenly sized, absent from sides of jaw, inner row very small, close-set and pointed.	Skin pigmentation below midlateral spots present.
Upper jaw teeth in 2–3 rows. In males teeth in outer row long, evenly sized and evenly spaced, fairly straight and slightly flattened with pointed tips, while in females, upper jaw teeth of small to medium length (not as long as in males), compressed, slender, teeth often close-set but may be slightly apart, tips blunt or sharp.	Skin pigmentation below midlateral spots present.
Upper jaw teeth in 2–3 rows, teeth in outer row always largest, stout and conical, curved to fairly straight with slightly pointed to almost blunt tips; teeth in inner rows very small, close-set and sharp. Teeth smaller in females.	Skin pigmentation below midlateral spots present.
Upper jaw teeth in 2 rows. In males teeth in outer row largest and widely spaced, slightly flattened and usually straight with pointed tips; in females, outer row teeth very small, close-set, evenly sized and usually blunt-tipped.	Skin pigmentation below midlateral spots present.
Upper jaw teeth in 2 rows. In males teeth in outer row evenly spaced, compressed, with bluntly pointed tips; in females, outer row teeth compressed, blunt-tipped and closely-set.	Skin pigmentation below midlateral spots present.
Upper jaw teeth in 2–3 rows. In males teeth in outer row slightly flattened, tips blunt or rounded, with two small curved symphyseal canines behind anterior tooth rows; females with outer row teeth of upper jaw small, compressed, evenly sized and blunt-tipped.	Skin pigmentation below midlateral spots present.
In both sexes upper jaw teeth in 2–4 rows, very small, sharp and close-set, outer row teeth larger.	Skin pigmentation below midlateral spots present.
Upper jaw teeth in 2–6 rows. In males teeth in outer row always largest, slightly curved, conical to slightly flattened; in females outer row of upper jaw teeth variable, may be similar to males with two rows of upright slightly flattened teeth, or row of short compressed blunt to pointed teeth.	Skin pigmentation below midlateral spots present.
In both sexes upper jaw teeth very small, straight and sharp, in 2–3 evenly sized rows. Lower jaw teeth in 2–3 rows, but teeth smaller and blunter.	Melanophores at midlateral at best grouped as individual distinct dots.
Upper jaw teeth in 2–3 rows, teeth in outer row stout and conical, curved to fairly straight with slightly pointed to almost blunt tips. Teeth smaller in females.	Skin pigmentation below midlateral spots present.
Upper jaw teeth in 3–4 rows, teeth in outer row always largest and usually widely spaced, conical to slightly flattened, fairly straight with slightly pointed tips (tips may be honey-coloured); some females have outer row teeth very small.	Skin pigmentation below midlateral spots present.
In both sexes upper jaw in 2–3 rows, teeth in outer row slender, slightly curved and pointed.	Skin pigmentation below midlateral spots present.
Upper jaw teeth in 2–3 rows. In males teeth in outer row large, widely spaced, conical, fairly straight with slightly pointed tips; in females, upper jaw teeth small, evenly sized and sharp.	Skin pigmentation below midlateral spots present.
Upper jaw in 2 rows. In males, teeth in outer row largest and widely spaced, usually straight with pointed tips, smaller teeth may alternate with larger; in females, outer row teeth very small, close-set, evenly sized and blunt-tipped to tips somewhat rounded.	Skin pigmentation below midlateral spots present.

data vs. Larson & Hammer 2021): scales in transverse series 7 vs. 8 in *P. minimus*; predorsal scale count 4–6 vs. 8–10 in *P. minimus*; the first spine longest in adults, the first spine equal in length to the second spine in juveniles vs. first dorsal fin rounded, second or third spines longest in *P. minimus*; interorbital width in head length 8.4–11.3 % vs. 11.1–17.4 % in *P. minimus*; anterior end of suborbital sensory papillae row *b* positioned below posterior iris vs. anterior end of row *b* positioned below pupil in *P. minimus* (see Fig. 7 vs. fig. 20 and text in Larson & Hammer 2021); anterior end of suborbital sensory papillae row *d* extending anteriorly just to above upper lip near angle of jaws, preorbital rows *jc* and *jd* absent vs. papillae in continuous row from row *d* to row *ja*, probably by the presence and connection of rows *jc* and *jd* to row *d* in *P. minimus* (see Fig. 7 vs. fig. 20 and text in Larson & Hammer 2021). Finally, the new species is only known from the Persian Gulf, whereas *P. minimus* was recorded from Chilika and Pulicat lakes and the Sundarbans, India, and Sind, Pakistan (Larson & Hammer 2021).

Discussion

The mtDNA sequences of the snubnose gobies from the most western part of the Indian Ocean (Persian Gulf) strongly suggest that our current knowledge severely underestimates the number of species of the genus *Pseudogobius*, an inference which was already put forward by Hammer et al. (2021). The mtDNA genetic data presented here allowed confident identification of candidate snubnose goby species in the Persian Gulf and they provided a broader phylogenetic framework that flags likely relationships of species distributed in Australia and Asia. Up to now, Hammer et al. (2021), Larson & Hammer (2021) and this study demonstrated that genus *Pseudogobius* is a hyper-cryptic species complex with high levels of endemism across its wider geographical distribution. This makes *Pseudogobius* as a good candidate for biogeographical studies. As illustrated in the phylogenetic tree, *P. youtabae*, *P. masago*, and *P. minimus* make up a distinct clade, and *P. youtabae* (which was preliminary identified as *P. masago*) is the sister group to *P. minimus*, with a comparatively low genetic distance of 10 %. This phylogenetic closeness is also mirrored by morphological characteristics.

The new species represents the smallest *Pseudogobius* species: it features the smallest recorded adult size of any *Pseudogobius* species, since specimen paratype male PMR VP5879 has length of only 13.4 +3.6 mm; and by the largest known specimen, the paratype female PMR VP5876 measured only 15.4 + 4.4 mm. Among *Pseudogobius*, only its sister species *P. minimus* has a more reduced pigmentation pattern in preserved material, and, with a SL of 18 mm, it was the *Pseudogobius* with the smallest maximum know size until the discovery of the new species described herein. Both these miniature *Pseudogobius* species are less richly coloured, compared with congeners. The shape of the urogenital papillae of *Pseudogobius* species differ from the common shape of gobiid urogenital papillae, both for males and females, including shapes reported for *Pseudogobius* species by Larson & Hammer (2021) (Fig. 3). In the Mediterranean, the smallest species of the genus *Pomatoschistus*, *P. nanus* Engin & Seyhan Öztürk, 2017, also was described as having an unusual urogenital papilla shape, albeit just in females, whereas other *Pomatoschistus* species have males with the common elongate papilla typical for gobiid males, and females with a short and broad papilla, typical for goby females, (Engin & Seyhan 2017). In addition to urogenital papilla, males and females of the new species were sexually dimorphic with regard to differences in non-overlapping morphometrics (Table 3): males have a more robust body and caudal peduncle, although the value for the caudal peduncle depth of the juvenile male slightly overlaps with the values in females. In addition, values of the character snout length in eye diameter was non-overlapping between sexes; and, finally, the rearward extension of pelvic fin posterior end was clearly different between males and females. The shape of urogenital papilla in paratype juvenile female ZM-CBSU py001 was more simple that of adult females, i. e., with less prominent medial indentation, a less prominent bifurcated posterior edge and a clearly visible opening. The juvenile female urogenital papilla was therefore less different from the male shape than that of adult females. The paratype juvenile male ZM-CBSU py002 had the shape of urogenital papilla resembling the adult male shape. In addition, the paratype juvenile female ZM-CBSU py001 had no completely enclosed head sensory canals.

Snubnose gobies of the genus *Pseudogobius* are ubiquitous to, and important elements of estuarine ecosystems of the Indo-West Pacific. These small benthic fishes occur in freshwater (e. g., *P. olorum* and *P. melanosticta*), brackish (e. g., *P. minimus* and *P. poicilosoma* (Bleeker, 1849)) and marine habitats (e. g., *P. rhizophora* and *P. youtabae*) such as sheltered tide pools, mangroves, and lowland streams above tidal influence (Hammer et al. 2021, Larson & Hammer 2021). They are often abundant, found over muddy, silty and sandy substrates, in seagrass beds, rocky areas and mangroves, and thus appear to be tolerant of a wide range of environmental conditions (Larson & Hammer 2021). Up to date, *P. youtabae* has

been found in the intertidal area on a sandy-muddy substrate near the mangrove protected area of Qeshm Island (Persian Gulf). No freshwater population of this species is known, yet. However, due to its small size more surveys are needed to locate other populations. Its phylogenetically closest relative, *P. minimus*, is found in coastal brackish lagoons, known only from brackish lakes and salt pans in Chilika and Pulicat lakes and the Sundarbans, India, and Sind, Pakistan (Larson & Hammer 2021).

The present species description increases the number of valid *Pseudogobius* species to 16 (Larson & Hammer 2021). Most *Pseudogobius* species of the genus have a restricted distribution in the west Pacific (Larson & Hammer 2021; this study). Only four species, *P. fulvicaudus*, *P. youtabae*, *P. minimus* and *P. melanosticta* occur in Indian Ocean, reaching on west to Iran, the eastern Pakistan and south India, respectively (present research, Larson & Hammer 2021, Ragul et al. 2024). Among those, *P. youtabae* and *P. minimus* are Indian Ocean endemics. *Pseudogobius youtabae* has the westernmost distribution of any known *Pseudogobius* species, non-overlapping with other *Pseudogobius* species, and it is the only known species known from the Persian Gulf.

Acknowledgements

We would like to thank Yeganeh Sadeghi (Shiraz University) for helping with fish collection, and Hasan Hashemi (Department of Environment of Hormuzgan) for providing collection facilities. We thank Helen K. Larson (Museum of Tropical Queensland) for her valuable comments and data provided on the genus *Pseudogobius* and its species, and Michael P. Hammer (Museum and Art Gallery of the Northern Territory, Darwin) for providing available literatures. This work is based upon research funded by Iran National Science Foundation (INSF), Project No. 4034780, granted to HRE. HRE and VS have been supported by the Shiraz University grant (SU-9831510), and MK has been supported by the grant of the Croatian Science Foundation under the project IP-2022-10-7542.

References

Darriba, D., Taboada, G. L., Doallo, R. & Posada, D. 2012. "jModelTest 2: more models, new heuristics and parallel computing". Nature Methods 9(8): 772.

Engin, S. & Seyhan, D. 2017. A new species of *Pomatoschistus* (Teleostei, Gobiidae): the Mediterranean's smallest marine fish. Journal of Fish Biology 91: 1208–1223.

Hall, T. A. 1999. BioEdit: a user-friendly biological sequence alignment editor and analysis program for Windows 95/98/NT. Nucleic Acids Symposium Series 41: 95–98.

Hammer, M. P., Adams, M., Unmack, P. J., Hassell, K. L. & Bertozzi, T. 2021. Surprising *Pseudogobius*: molecular systematics of benthic gobies reveals new insights into estuarine biodiversity (Teleostei: Gobiiformes). Molecular Phylogenetics and Evolution 160: 107140.

Hubbs, C. L. & Lagler, K. F. 1958. Fishes of the Great Lakes region. 545 pp., Ann Arbor, Michigan (University of Michigan Press).

Huelsenbeck, J. P. & Ronquist, F. 2001. MrBayes: Bayesian inference of phylogeny. Bioinformatics 17: 754–755.

Kovačić, M. & Svensen, R. 2024. Revision of Sanzo's head lateral-line system (HLLS) classification and nomenclature based on its re-evaluation of almost all native Mediterranean and European Atlantic marine gobies. Spixiana 46: 229–295.

Larson, H. K. & Hammer, M. P. 2021. A revision of the gobiid fish genus *Pseudogobius* (Teleostei, Gobiidae, Tridentigerinae), with description of seven new species from Australia and South-East Asia. Zootaxa 4961: 1–85.

Posada, D. & Crandall, K. A. 1998. MODELTEST: testing the model of DNA substitution. Bioinformatics 14: 817–818.

Ragul, S., Manoj, A., Mahadevan, G., Murugan, A. & Larson, H. K. 2024. First record of two gobioid fishes (Perciformes: Gobiidae) from Indian waters. Journal of the Marine Biological Association of the United Kingdom 104: e35.

Saruwatari, T., Andres Lopez, J. & Pietsch, T. W. 1997. Cyanine blue: a versatile and harmless stain for specimen observation. Copeia 1997(4): 840–841.

Stamatakis, A. 2006. RAxML-VI-HPC: maximum likelihood-based phylogenetic analyses with thousands of taxa and mixed models. Bioinformatics 22: 2688–2690.

Tamura, K., Stecher, G., Peterson, D., Filipski, A. & Kumar, S. 2013. MEGA6: Molecular Evolutionary Genetics Analysis version 6.0. Molecular Biology and Evolution 30: 2725–2729.

Ward, R. D., Zemlak, T. S., Innes, H. B., Last, R. P. & Hebert, P. D. N. 2005. DNA barcoding Australia's fish species. Philosophical Transactions of the Royal Society of London, Series B, Biological Sciences 360(1462): 1847–1857.